1
Magnetism

Maria Bałanda and Robert Pełka

1.1
Origin of Magnetism

In magnetism, an object of fundamental importance is the magnetic moment [1]. In the framework of classical electrodynamics, an elementary magnetic moment is equivalent to a current loop. If there is a current around a negligible oriented loop of area $|\mathrm{d}\mathbf{S}|$, then the magnetic moment associated with this current amounts to

$$\mathrm{d}\boldsymbol{\mu} = I\ \mathrm{d}\mathbf{S}, \tag{1.1}$$

which implies that the magnetic moment is expressed in ampere square meter. The length of the pseudo-vector $\mathrm{d}\mathbf{S}$ is equal to the area of the loop, its direction is perpendicular to the loop, and its sense coincides with the orientation of the current around the elementary loop. Thus, the magnetic moment points normal to the loop of current and hence can be either parallel or antiparallel to the angular momentum associated with the charge going round the loop and producing the current (see Figure 1.1). The orbiting electrical charges considered in solid-state physics are all associated with particles carrying mass. Therefore, besides the orbital motion of charge, there is an orbital motion of mass implying that a magnetic moment is always connected with angular momentum. In atoms, the magnetic moment $\boldsymbol{\mu}$ associated with an orbiting electron shows the same direction as the angular momentum $\mathbf{L}$ of the electron, and is linearly proportional to it:

$$\boldsymbol{\mu}_{\mathbf{L}} = \gamma_{\mathrm{L}}\mathbf{L}, \tag{1.2}$$

where γ_{L} is a constant called the gyromagnetic ratio. This relationship between the magnetic moment and the angular momentum is demonstrated by two related phenomena: the Einstein–de Haas effect, where rotation is induced by magnetization, and the Barnett effect, where the reverse is the case.

The energy of the magnetic moment $\boldsymbol{\mu}$ in a magnetic field $\mathbf{B}$ is given by

$$E = -\boldsymbol{\mu}\cdot\mathbf{B} \tag{1.3}$$

Hence, the energy attains a minimum value when the magnetic moment is parallel to the magnetic field. Beyond the state corresponding to the minimum energy,

Molecular Magnetic Materials: Concepts and Applications, First Edition.
Edited by Barbara Sieklucka and Dawid Pinkowicz.

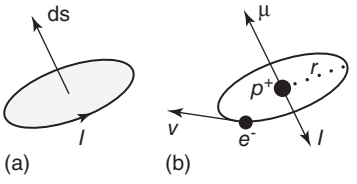

Figure 1.1 An elementary magnetic moment $d\boldsymbol{\mu} = I\,d\mathbf{S}$ due to an elementary current loop (a). An electron in a hydrogen atom orbiting with velocity **v** around the nucleus (a single proton) giving rise to the magnetic moment $\boldsymbol{\mu}$ antiparallel to its orbital angular momentum **l** (b).

there is a torque on the magnetic moment given by

$$\mathbf{G} = \boldsymbol{\mu} \times \mathbf{B} \tag{1.4}$$

Since the magnetic moment is associated with the angular momentum **L** by Eq. (1.2), and because torque is equal to rate of change of angular momentum, Eq. (1.4) implies

$$\frac{d\boldsymbol{\mu}}{dt} = \gamma \boldsymbol{\mu} \times \mathbf{B}. \tag{1.5}$$

According to Eq. (1.5), the change of $\boldsymbol{\mu}$ is perpendicular to both $\boldsymbol{\mu}$ and **B**. Hence, rather than turning the magnetic moment toward the magnetic field, the latter causes the direction of $\boldsymbol{\mu}$ to precess around **B**. This equation also implies that the magnitude $|\boldsymbol{\mu}|$ is time-independent. This situation is exactly analogous to the spinning of a gyroscope or spinning top. The precession frequency called the Larmor precession frequency is equal to $|\gamma \mathbf{B}|$. This feature distinguishes the magnetic moment from the electric dipole in an electric field. A stationary electric dipole moment is not associated with any angular momentum; therefore, if it is not aligned with the electric field, there is a torque tending to turn the direction of the dipole toward the electric field.

One can easily estimate the characteristic size of atomic magnetic moments. Consider an electron (charge $-e$, mass m_e) performing a circular orbit around the nucleus of a hydrogen atom (the Bohr model, see Figure 1.1b). The current I around the atom is $I = -e/T$, where $T = 2\pi r/v$ is the orbital period, $v = |\mathbf{v}|$ is the speed, and r is the radius of the circular orbit. The magnitude of the angular momentum of the electron, $m_e vr$, must be equal to $\hbar$ in the ground state, so that the magnetic moment of the electron is

$$\mu = \pi r^2 I = -\frac{e\hbar}{2m_e} \equiv -\mu_B, \tag{1.6}$$

where μ_B is the Bohr magneton, whose value equals 9.274×10^{-24} A m^2. This is a convenient unit for describing the size of atomic magnetic moments. Note that sign of the magnetic moment in Eq. (1.6) is negative. Because of the negative electronic charge, its magnetic moment is antiparallel to its angular momentum. The gyromagnetic ratio associated with the orbital motion of an electron is hence $\gamma_L = \mu/\hbar = -e/2m_e$. The Larmor frequency is then $\omega_L = |\gamma| B = eB/2m_e$.

In addition to the orbital angular momentum of an orbiting electron, there is an intrinsic angular momentum called spin momentum, introduced by Uhlenbeck and Goudsmit in 1925 to explain the existing spectroscopic observations. The splitting of many spectral lines in the magnetic field (the so-called anomalous

Zeeman effect) can be rationalized only if an electron possesses the spin angular momentum $\hbar\mathbf{s}$. It was experimentally verified and theoretically confirmed that magnetic moment associated with the spin angular momentum is given by

$$\boldsymbol{\mu}_s = -g_s \frac{e}{2m_e}\hbar\mathbf{s}, \tag{1.7}$$

with $g_s = 2(1 + \alpha/2\pi + \cdots) \approx 2.0023$, where $\alpha = 1/137.04$ is the fine structure constant. Hence, the gyromagnetic ratio associated with the spin angular momentum is $\gamma_s = -g_s e/2m_e$. The fact that in the case of the spin magnetic moment an additional factor $g_s \approx 2$ occurs, which is absent for orbital magnetic moment, is called the gyromagnetic anomaly.

The orbital angular momentum in a real atom depends on the electronic state occupied by the electron. With quantum numbers l and m_l, the component of orbital angular momentum along a fixed axis (usually the z-axis) is $m_l\hbar$ and the magnitude of the orbital angular momentum is $\sqrt{l(l+1)}\hbar$. Thus, the component of magnetic moment along the z-axis is $-m_l\mu_B$ and the magnitude of the total magnetic dipole moment is $\sqrt{l(l+1)}\mu_B$. The spin of an electron is characterized by a spin quantum number s, which for an electron takes the value 1/2. The component of spin angular momentum is $m_s\hbar$ with only two possible values of $m_s = \pm 1/2$. The component of angular momentum along a particular axis is then $\hbar/2$ or $-\hbar/2$. These alternatives are referred to as "up" and "down," respectively. The magnitude of the spin angular momentum for an electron is $\sqrt{s(s+1)}\hbar = \sqrt{3}\hbar/2$. The component of magnetic moment associated with spin along a particular axis is equal to $-g_s\mu_B m_s$ and its magnitude is $\sqrt{s(s+1)}g_s\mu_B = \sqrt{3}g_s\mu_B/2$. In general, both orbital and spin angular momenta for electrons in atoms combine to form total angular momentum $\hbar\mathbf{J}$. The resultant magnetic moment is then given by

$$\boldsymbol{\mu}_J = -g_J \frac{e}{2m_e}\hbar\mathbf{J}, \tag{1.8}$$

where the Landé factor g_J can take different values depending on the relative contributions of spin and orbital angular momenta. It is equal to 1 for the pure orbital contribution and 2 for the pure spin contribution. This point will be discussed later in more detail.

1.2 Macroscopic Approach

A piece of magnetic solid consists of a large number of atoms with magnetic moments. A macroscopic characteristic of the intensity of magnetism in a solid is given by the magnetization $\mathbf{M}$ defined as the magnetic moment per unit volume. This quantity is usually considered in the continuum approximation, that is, on a length scale large enough to disregard the graininess due to the individual atomic magnetic moments. $\mathbf{M}$ is thus considered a smooth vector field, continuous everywhere except at the edges of the magnetic solid.

Although free space (vacuum) fails to have any magnetization, it can accommodate a nonzero magnetic field. The magnetic field is described by the vector fields **B** (called magnetic induction) and **H** (called magnetic field strength) related by

$$\mathbf{B} = \mu_0 \mathbf{H}, \tag{1.9}$$

where $\mu_0 = 4\pi \times 10^{-7}\,\mathrm{H\,m^{-1}}$ is the permeability of free space. The two magnetic fields **B** and **H** are just scaled versions of each other, the former measured in tesla (abbreviated to T) and the latter measured in amperes per meter. In a magnetic solid, the general relationship is

$$\mathbf{B} = \mu_0(\mathbf{H} + \mathbf{M}), \tag{1.10}$$

and the relationship between **B** and **H** is more complicated and the two vector fields may be very different in magnitude and direction. In the special case that the magnetization **M** is linearly related to the magnetic field **H**, the solid is called a linear material, and the constant dimensionless proportionality factor χ is called the magnetic susceptibility, and hence we may write

$$\mathbf{M} = \chi \mathbf{H}. \tag{1.11}$$

In this special case, the relationship between **B** and **H** is still linear, that is

$$\mathbf{B} = \mu_0(1 + \chi)\mathbf{H} = \mu_0 \mu_r \mathbf{H}, \tag{1.12}$$

where $\mu_r = 1 + \chi$ is the relative permeability of the material.

For the sake of argument, consider a region of free space with an applied magnetic field given by fields $\mathbf{B}_a$ and $\mathbf{H}_a$, where $\mathbf{B}_a = \mu_0 \mathbf{H}_a$. On inserting a magnetic solid into the region of free space, the internal fields inside the solid, given by $\mathbf{B}_i$ and $\mathbf{H}_i$, can very much differ from $\mathbf{B}_a$ and $\mathbf{H}_a$, respectively. Due to the magnetic field produced by all magnetic moments in the solid, both $\mathbf{B}_i$ and $\mathbf{H}_i$ will depend on the position inside it at which they are measured. This is true except in the special case of an ellipsoid-shaped sample, where if the magnetic field is applied along one of the principal axes of the ellipsoid, then everywhere inside the sample

$$\mathbf{H}_i = \mathbf{H}_a - N\mathbf{M}, \tag{1.13}$$

where N is the appropriate demagnetizing factor. The term $\mathbf{H}_d = -N\mathbf{M}$ is called the demagnetizing field. When the magnetization is large compared to the applied field (measured before the sample was inserted), these demagnetizing corrections need to be taken seriously. For the special case of weak magnetism, where $\chi \ll 1$, $M \ll H$, $H_i \approx H_a$, and $B_i \approx \mu_0 H_i$, we can neglect the demagnetizing correction. However, in ferromagnets, demagnetizing effects are always significant. Therefore, a comment is in order here. Experimental measurement gives the ratio of magnetization M and an applied field H_a:

$$\chi_{\mathrm{exp}} = \frac{M}{H_a}. \tag{1.14}$$

This quantity will in general differ from the intrinsic magnetic susceptibility of a material given by

$$\chi_{\mathrm{int}} = \frac{M}{H_i}. \tag{1.15}$$

The two quantities are related by

$$\chi_{\text{exp}} = \frac{M}{H_{\text{i}} + NM} = \frac{\chi_{\text{int}}}{1 + N\chi_{\text{int}}}. \tag{1.16}$$

When $\chi_{\text{int}} \ll 1$, there is little distinction between χ_{int} and χ_{exp}. By contrast, when χ_{int} is closer to or above 1, the distinction can be very significant. For example, in a ferromagnet approaching the Curie temperature from above, $\chi_{\text{int}} \to \infty$, but $\chi_{\text{exp}} \to 1/N$.

1.3 Units in Magnetism

The SI system of units (Système International d'Unités) is the legal one, but as Olivier Kahn rightly remarked, legality is not science. In fact, most researchers involved in the field of molecular magnetism prefer to use the **cgs emu** system. In the cgs system, distance, mass, and time are measured in centimeters, grams, and seconds, respectively. The unit of magnetic field (**H**) in the system is oersted (Oe), and the unit of magnetic induction (**B**) created by the magnetic field of 1 Oe is 1 G. In vacuum, **B** is related to **H** through Eq. (1.9), where the permeability μ_0 in the cgs emu system is equal to 1. The counterpart of Eq. (1.10) in the cgs emu system is the relation $\mathbf{B} = \mathbf{H} + 4\pi\mathbf{M}$. The magnetic moment is measured in units failing to carry a specific name and hence referred to as emu (simple representation of "electromagnetic unit"). The definition of 1 emu of magnetic moment can be clarified by considering a magnet placed in an external magnetic field **B**. Such a magnet will experience a torque given by Eq. (1.4), which implies that the magnitude of the torque depends crucially on the orientation of the magnet with respect to the magnetic field. There are actually two oppositely directed orientations, in which the magnet will experience the maximum torque. The magnitude of the magnetic moment is defined as *the maximum torque experienced by the magnet when placed in unit external magnetic field*. Hence, the cgs emu unit for magnetic moment is clearly dyne centimeter per gauss, where dyne is the unit of force (dyne = g cm s^{-2}). As dyne cm = erg (the unit of energy), emu of magnetic moment = erg G^{-1}. The volume magnetic susceptibility (see Eq. (1.11)) is dimensionless and traditionally expressed in electromagnetic unit per cubic centimeter, such that the dimension of emu is formally cubic centimeter. Therefore, the molar magnetic susceptibility is expressed in cubic centimeter per mole. The magnetization is defined as the magnetic moment per unit volume and is expressed in oersted or electromagnetic unit per cubic centimeter. The molar magnetization can be expressed in either cubic centimeter oersted per mole or $N_{\text{A}}\mu_{\text{B}}$ units, where N_{A} is Avogadro's number and μ_{B} is the Bohr magneton. The relationship between the two units is: $1N_{\text{A}}\mu_{\text{B}} = 5585\ \text{cm}^3\ \text{Oe mol}^{-1}$. Table 1.1 summarizes the relevant quantities expressed in the SI system and the cgs emu system together with appropriate conversion factors.

For a paramagnet, the molar susceptibility χ_{m} is given by Curie's law (see Eq. (1.33)), which expressed in terms of the effective moment in SI units acquires

Table 1.1 Units in the SI system and cgs emu system.

Quantity	Symbol	SI unit	cgs emu unit
Length	X	10^{-2} m	=1 cm
Mass	m	10^{-3} kg	=1 g
Force	$\mathbf{F}$	10^{-5} N	=1 dyne
Energy	E	10^{-7} J	=1 erg
Magnetic induction	$\mathbf{B}$	10^{-4} T	=1 G
Magnetic field strength	$\mathbf{H}$	$10^3/4\pi$ A m^{-1}	=1 Oe
Magnetic moment	$\mathbf{M}$	10^{-3} J T^{-1} or A m^2	=1 erg G^{-1} or emu
Magnetization(=moment per volume)	$\mathbf{M}$	10^3 A m^{-1} or J T^{-1} m^{-3}	=1 Oe or emu cm^{-3}
Magnetic susceptibility	χ	$4\pi \times 1$	=1 emu cm^{-3} or emu cm^{-3} Oe^{-1}
Molar susceptibility	χ_{m}	$4\pi \times 10^{-6}$ m^3 mol^{-1}	=1 emu mol^{-1} or emu mol^{-1} Oe^{-1}
Mass susceptibility	χ_{g}	$4\pi \times 10^{-3}$ m^3 kg^{-1}	=1 emu g^{-1} or emu g^{-1} Oe^{-1}
Magnetic flux	Φ	10^{-8} T m^2 or Wb	=1 G cm^2 or Mx
Demagnetization factor	N	$0 < N < 1$	$0 < N < 4\pi$

m, meter; g, gram; N, newton; J, joule; T, tesla; G, gauss; A, ampere; Oe, Oersted; Wb, Weber; Mx, Maxwell.

the form

$$\chi_{\mathrm{m}} = \frac{\mu_0 N_{\mathrm{A}} \mu_{\mathrm{eff}}^2 \mu_{\mathrm{B}}^2}{3k_{\mathrm{B}}T}. \tag{1.17}$$

Hence, $\chi_{\mathrm{m}}T$ is independent of temperature and is related to the effective moment through the equation $\mu_{\mathrm{eff}} = [3k_{\mathrm{B}}/\mu_0 N_{\mathrm{A}}\mu_{\mathrm{B}}^2]^{1/2}\sqrt{\chi_{\mathrm{m}}T}$, so that

$$\mu_{\mathrm{eff}} = 797.8\sqrt{\chi_{\mathrm{m}}^{\mathrm{SI}}T} \approx 800\sqrt{\chi_{\mathrm{m}}^{\mathrm{SI}}T} \quad \text{(SI)} \tag{1.18}$$

$$\mu_{\mathrm{eff}} = 2.827\sqrt{\chi_{\mathrm{m}}^{\mathrm{cgs}}T} \approx \sqrt{8\chi_{\mathrm{m}}^{\mathrm{cgs}}T} \quad \text{(cgs emu)}, \tag{1.19}$$

where μ_{eff} is measured in Bohr magnetons per formula unit, $\chi_{\mathrm{m}}^{\mathrm{SI}}$ in cubic meter per mole, and $\chi_{\mathrm{m}}^{\mathrm{cgs}}$ is measured in electromagnetic unit per mole.

1.4 Ground State of an Ion and Hund's Rules

A typical atom contains many electrons, majority of which reside in filled shells with no net angular momentum. However, there may be unfilled shells and the electrons in these shells combine to give nonzero spin and orbital angular momenta. For atoms with high atomic number Z, the spin–orbit interaction energy ($\sum_i \lambda_i \mathbf{l}_i \cdot \mathbf{s}_i$, where index i enumerates the electrons in unfilled shells) is the dominant energy compared with the electrostatic interactions and therefore

cannot be treated as a small perturbation. In this case, one has to couple the spin and orbital angular momentum of each electron separately, and consequently the weaker electrostatic effect may then couple the total angular momentum from each electron. This type of scheme of determining the ground state of an atom or ion is called **j**–**j** coupling. Far more frequently, another scheme known as **L**–**S** coupling or Russell–Saunders coupling is effective, where the reverse is the case, that is, the spin–orbit interaction may be treated as a weak perturbation of the main energy terms determined by the electrostatic interactions. The latter terms control the values of total orbital angular momentum $\hbar\mathbf{L}$ originating from the combination of all the orbital angular momenta of the electrons in the unfilled shells and total spin angular momentum $\hbar\mathbf{S}$ being the result of the combination of all their spin angular momenta. The different configurations corresponding to different possible values of L and S quantum numbers will cost different amounts of energy. The choice of spin angular momentum affects the spatial part of the total atomic wavefunction and the orbital angular momentum affects how the electrons travel around the nucleus affecting the electrostatic repulsion energy. Furthermore, the spin and orbital angular momenta weakly couple via the spin–orbit interaction ($\lambda\mathbf{L}\cdot\mathbf{S}$) giving rise to the total angular momentum $\mathbf{J}=\mathbf{L}+\mathbf{S}$ being a conserved quantity and an (L, S) multiplet being split into a number of levels with differing J quantum number.

The combination of angular momentum quantum numbers, which minimize the energy, can be estimated using empirical rules listed in order of decreasing importance known as Hund's rules [2].

a) Maximize S in the way compatible with the Pauli exclusion principle. With l being the orbital quantum number of the partially completed shell and p the number of electrons within this shell (i.e., $p < 2(2l+1)$), one obtains

$$S = \frac{1}{2}[(2l+1) - |2l+1-p|] \tag{1.20}$$

b) Maximize L in the way compatible with the Pauli exclusion principle and rule (a). L is given by

$$L = S\cdot|2l+1-p| \tag{1.21}$$

c) Finally, the value of J is found using $J=|L-S|$ if the shell is less than half-full ($p \le 2l+1$) and $J=L+S$ if it is more than half-full ($p \ge 2l+1$). This can be written as

$$J = S\cdot|2l-p|. \tag{1.22}$$

The third rule arises from an attempt to minimize the spin–orbit energy. The scope of applicability of the third rule is limited to certain circumstances. While it works very well for rare earth ions, the spin–orbit energies loose on their significance in the case of transition metal ions where the crystal field effects become dominant.

The configuration which is found using Hund's rules is described using a term symbol of the form ${}^{2S+1}L_J$ with $2S+1$ named multiplicity, and $L=0,1,2,\ldots$ labeled

by subsequent letters $S, P, D, F, G, \ldots$. Generally, Hund's rules enable to predict the ground state of an atom or ion; however, they are not suited to describe any excited state or its distance from the ground state. Reliable estimations of the magnetic moment of an ion confine to those cases where only the ground state is populated. The predictions of the orbital angular momentum quantum number L, the spin angular momentum quantum number S, and the total angular momentum quantum number J for the magnetically relevant 3d ions (transition metals Sc–Zn) and 4f ions (lanthanides La–Lu) are shown in Figure 1.2.

Given the quantum numbers L, S, and J, the ground state of an ion is defined. Equation (1.8) gives the corresponding magnetic moment of that state, where the Landé g_J factor can be shown as

$$g_J = \frac{3}{2} + \frac{S(S+1) - L(L+1)}{2J(J+1)}. \tag{1.23}$$

Thus, the magnitude of the magnetic moment is given by

$$\mu = \mu_B g_J \sqrt{J(J+1)}. \tag{1.24}$$

It should be compared with the effective magnetic moment determined in the susceptibility measurement. An extremely good experimental agreement is found between this prediction and the measured values for 4f ions in the solid state. A discrepancy occurs for Sm and Eu, which is due to the low-lying excited states with different J from the ground states. Much poorer agreement is found for the 3d ions because of the effect of the local crystal environment.

The competition between the electrostatic interaction and the spin–orbit coupling in an atom or ion determines the splitting of the energy states and specifies the ground state. The ensuing structure of the energy spectrum (states characterized by L and S are split into a number of levels with differing J) is known as fine structure. However, not only the electrons in an atom have magnetic moment. The nucleus often has a nonzero spin defined by the nuclear spin quantum number

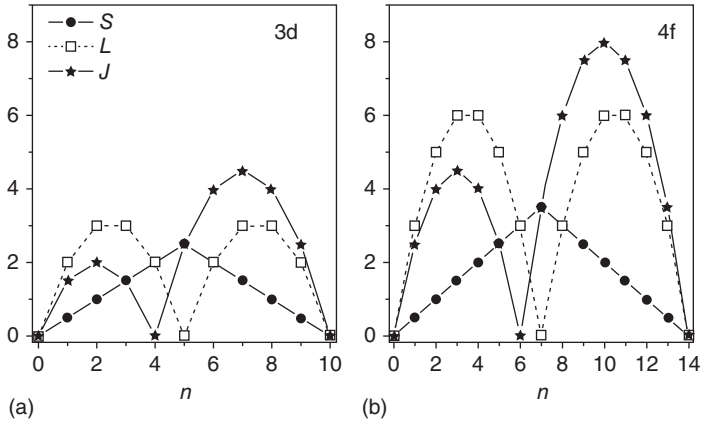

Figure 1.2 S, L, and J for (a) 3d and (b) 4f ions according to Hund's rules (n is the number of electrons in the corresponding subshell).

I, taking both integer and half-integer values and representing the total angular momentum of the nucleus in units of $\hbar$. The unit of nuclear magnetism is the nuclear magneton μ_N given by

$$\mu_N = \frac{e\hbar}{2m_p} = 5.0508 \times 10^{-27}\,\mathrm{A\,m^2}, \tag{1.25}$$

where m_p is the mass of the proton. This is three orders of magnitude smaller than the typical electronic magnetic moment given by the Bohr magneton μ_B. The magnetic moment of a nucleus takes a value of

$$\mu = g_I \mu_N \sqrt{I(I+1)}, \tag{1.26}$$

where g_I is the nuclear g-factor, which is a number of order of unity reflecting the detailed structure of the nucleus. The nuclear moment can magnetically interact with the electronic moment, but the interaction is very weak. This leads to energy splitting, which is even smaller than the fine structure, and hence known as hyperfine structure. The essential principles of its origin can be understood by considering a nuclear moment $\boldsymbol{\mu}$, which is subject to a magnetic field $\mathbf{B}_e$ produced by the motion and spin of all the electrons. This produces an energy term $-\boldsymbol{\mu} \cdot \mathbf{B}_e$, with $\mathbf{B}_e$ proportional to the total angular momentum of all the electrons $\mathbf{J}$, so that the Hamiltonian for the hyperfine interaction is usually written as

$$\hat{H}_{hf} = A\mathbf{I}\cdot\mathbf{J}. \tag{1.27}$$

Due to the relative weakness of this interaction, its effect on the magnetic properties of the solids becomes apparent only in the sub-kelvin range of temperatures.

1.5 An Atom in a Magnetic Field

For an isolated atom in a constant magnetic field $\mathbf{B}$, the Hamiltonian takes the form

$$\hat{H} = \hat{H}_0 + \mu_B(\mathbf{L} + g_s\mathbf{S})\cdot\mathbf{B} + \frac{e^2}{8m_e}\sum_i (\mathbf{B}\times\mathbf{r}_i)^2, \tag{1.28}$$

where $\hat{H}_0$ includes the electronic kinetic energy and potential energy. The second term describes the effect of the atom's own magnetic moment due to the presence of unpaired electrons and is known as the paramagnetic term. It is a dominant perturbation to the original Hamiltonian $\hat{H}_0$, but it sometimes vanishes leaving the sole contribution given by the third term and giving rise to the so-called diamagnetic moment, which is present even if the net magnetic moment of the atom vanishes. All materials show some degree of diamagnetism. The diamagnetic moment is directly proportional to the applied field and aligns antiparallel with it. It may be shown that the diamagnetic susceptibility is negative and for a spherically symmetric ion takes the general form

$$\chi = -\frac{N}{V}\frac{\mu_0 e^2}{6m_e}\sum_{i=1}^{Z}\langle r_i^2\rangle, \tag{1.29}$$

where N is the number of ions (each with Z electrons of mass m_e) in a solid of volume V and r_i is the magnitude of the position vector of the ith electron. The quantum mechanical average $\langle r_i^2 \rangle$ indicates that the effect crucially depends on the spatial extension of the filled atomic shells. This expression assumes first-order perturbation theory and zero absolute temperature. As the temperature is increased above zero, states above the ground state become progressively more important, but this is marginal effect. Diamagnetic susceptibilities are usually temperature-independent.

By contrast, paramagnetism is associated with a positive susceptibility, so that an applied magnetic field induces a magnetization aligning parallel with the applied magnetic field, which caused it. The nonzero magnetic moment on an atom is associated with its total angular momentum $\mathbf{J} = \mathbf{L} + \mathbf{S}$ and is given by Eq. (1.8). According to the Hamiltonian in Eq. (1.28), the energy of the atom in a magnetic field $\mathbf{B}$ taking the direction of the z-axis is

$$E = g_J \mu_B m_J B, \tag{1.30}$$

where $m_J = -J, -J+1, \ldots, J-1, J$. Using the methods of statistical physics, one can calculate the corresponding partition function, the free-energy thermodynamic potential, and finally the magnetization, which takes the form

$$M = n g_J \mu_B J B_J(x), \tag{1.31}$$

where n denotes the number of atoms in a unit volume, $x = g_J \mu_B J B / k_B T$, and $B_J(x)$ is the Brillouin function given by

$$B_J(x) = \frac{2J+1}{2J} \coth\left(\frac{2J+1}{2J} x\right) - \frac{1}{2J} \coth\left(\frac{x}{2J}\right). \tag{1.32}$$

At finite temperatures and for low magnetic fields, the Brillouin function can be approximated by its Maclaurin expansion, $B_J(x) = (J+1)x/3J + O(x^3)$, and the corresponding magnetic susceptibility is given by the formula

$$\chi = \frac{M}{H} \approx \frac{\mu_0 M}{B} = \frac{C}{T}, \tag{1.33}$$

where $C = n \mu_0 g_J {\mu_B}^2 J(J+1)/3k_B$ is the Curie constant and the expression amounts to the Curie law predicting an inversely proportional dependence on temperature.

If $J = 0$ in the ground state, then there is no paramagnetic effect in first-order perturbation theory. However, its second-order predicts a change in the ground-state energy, because it takes account of excited states with $J \neq 0$ being mixed in. The ensuing correction to the susceptibility is positive, small, and temperature independent, and is referred to as van Vleck paramagnetism.

1.6 Mechanisms of Magnetic Interactions

Magnetic solids may be classified into two basic, limiting models. The model of localized moments coming from electrons residing in an atomic or ionic shell

describes the magnetism of nonconducting materials. The other case is the ferromagnetism of metals, where the delocalized electrons may be responsible for both magnetism and charge transport. A bulk magnetic state with a long-range order and collective behavior of magnetic moments below a certain critical temperature T_c arises when there is a sufficiently strong magnetic interaction in the system. Localized magnetic moments interact via exchange or dipolar forces, while in the case of delocalized electrons, it is the exchange of spin-up and spin-down bands. The different types of magnetic interactions are described below [1, 3].

1.6.1 Dipolar Interactions

Apart from all interactions of the quantum mechanical origin itemized below, the mutual correlations between spins are governed by the classic dipolar interaction related to the field produced by particular magnetic moments. The energy of two parallel magnetic dipoles $\boldsymbol{\mu}_i$ and $\boldsymbol{\mu}_j$ separated by the distance r_{ij} is

$$E_{\text{dip}} = -\frac{\boldsymbol{\mu}_i \cdot \boldsymbol{\mu}_j [3\cos^2\alpha - 1]}{r_{ij}^3}, \tag{1.34}$$

where θ is the angle between direction of the moments and the vector connecting the dipoles. In opposite to exchange mechanisms, the dipolar interaction is long range ($\sim r^{-3}$), it does not need the overlap of orbitals, and works through space. E_{dip} is usually three orders of magnitude smaller than the exchange energy; taking $\mu = 1\mu_B$ and $r = 0.1\,\text{nm}$, one may expect magnetic order at $T_c \approx \mu^2/r^3 \approx 1\,\text{K}$. However, if the magnetic system consists of N exchange-correlated spin domains, dipolar forces may trigger magnetic ordering at a higher temperature of $T_c' \approx (N\mu)^2/r'^3$ [4]. Dipolar interaction is strongly anisotropic and the resultant energy depends on the shape of the object. Domain structure of ferromagnetic materials is the result of the tendency to minimize the dipolar interaction energy.

1.6.2 Direct Exchange

The dominant interaction leading to the collective state with the long-range order of localized magnetic moments in a solid is an exchange coupling. It is based on the tendency of reducing the electrostatic energy through separation in space charges of the same sign and on the Pauli exclusion principle for fermions, which states that the two electrons in the same spatial state cannot be in the same quantum state (say both spin-up). Consider the setup of two electrons with spins $\mathbf{S}_1$ and $\mathbf{S}_2$. If the energy of the setup in the singlet state (resultant spin $S = 0$) is E_S, and that of the triplet state (resultant spin $S = 1$) is E_T, then the so-called exchange integral is

$$J_{\text{ex}} = \frac{E_S - E_T}{2}, \tag{1.35}$$

and the spin dependent term in Hamiltonian is $H^{\text{spin}} = -J_{\text{ex}}\mathbf{S}_1 \cdot \mathbf{S}_2$. If $E_S > E_T$, the J_{ex} integral is positive and the magnetic coupling is ferromagnetic and the resultant

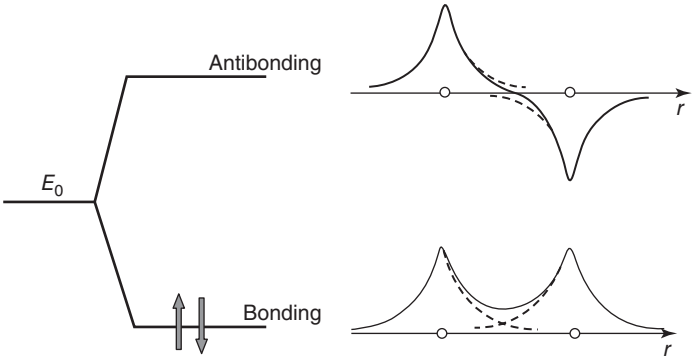

Figure 1.3 Spatially symmetric bonding orbital of a diatomic molecule with antiparallel spins and spatially antisymmetric antibonding molecular orbital.

spin $S = 1$; when $E_S < E_T$, the J_{ex} integral is negative, and coupling is antiferromagnetic with resultant $S = 0$.

In the system of many electrons, calculation of exchange integral is complicated, as mutual interactions of all electron pairs should be accounted for. Carriers of magnetic moments are spins of unpaired electrons residing on outer shell of atoms or ions. These electrons occupy the orbitals in such a way that the ground state adopts the highest value of the resultant spin that is allowed by the Pauli exclusion principle (Hund's rule). In a system of two or more atoms, the electrons interact due to the spatial overlap of the orbitals (*direct exchange*). Various configurations may arise: for the nonzero overlap integral, the *kinetic exchange* evokes an antiparallel alignment of spins, while in case of zero overlap integral, the *potential exchange* will tend the spins to align parallel. Figure 1.3 presents molecular orbitals for a diatomic molecule. The spatially symmetric bonding orbital, corresponding to the sum of the two atomic orbitals of energy E_0, comprises a nonzero electronic charge between the atoms. The electrons are coupled here antiparallel, in line with the rule for the total wavefunction (product of the space and spin components) for fermions, which should be antisymmetric. In general, the spatially symmetric orbital has the lowest energy, this is why the most probable state is a singlet with opposite spins. The spatially antisymmetric antibonding orbital, corresponding to the difference of the two atomic orbitals, contains a nodal plane with no charge between the atoms. For this case, the triplet state with parallel spin alignment is possible on condition of charge separation. As wavefunctions of electrons decay quickly with distance, exchange coupling decreases rapidly with the distance between metal-ion centers ($J_{ex} \sim r^{-10}$ [4]) and concerns mainly the nearest neighbors.

1.6.3
Indirect Exchange – Superexchange

In systems in which direct exchange cannot be realized due to insufficient overlap of magnetic orbitals, magnetic coupling may be mediated by orbitals of

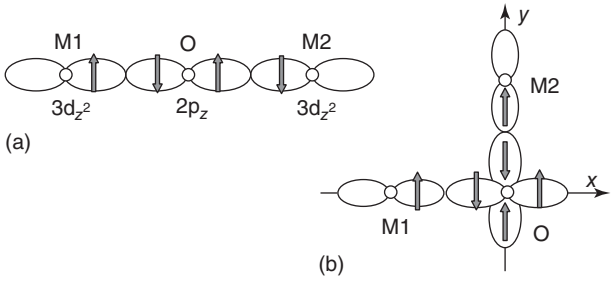

Figure 1.4 Superexchange interaction between metal ions mediated by the oxygen ligand. Dependent on the M1–O–M2 angle, the resulting coupling is antiferromagnetic (a) or weak ferromagnetic (b).

a nonmagnetic ligand (e.g., oxygen) located in between. It is the *superexchange interaction*, which is responsible for the magnetic properties of the most of magnetic materials, especially nonmetallic compounds, for example, oxides or fluorides. Like in the direct exchange, the mechanism of superexchange has two contributions: the weaker, *potential* one, which stabilizes ferromagnetic ground state through the orthogonal orbitals, and the *kinetic* one, preferring the antiferromagnetism, due to overlap of metal orbitals with ligand orbitals. The energy of the coupling depends on the electron configuration of magnetic ions and on the M1–O–M2 bond angle. The rules framed by Goodenough, Kanamori, and Anderson help predict the resulting coupling. In the case of singly occupied M1 and M2 3d obitals, one has (i) strong negative coupling when M1–O–M2 angle is equal to 180° (see Figure 1.4a); (ii) weak positive coupling for M1–O–M2 angle equal 90° (Figure 1.4b); and (iii) weak positive coupling occurs also if there is an empty orbital of M2 of other symmetry than that of M1 [5]. The Hubbard model describes the superexchange with energy U of Coulomb repulsion and with a matrix element t for the virtual hopping of the oxygen 2p electrons. If $U \ll t$, then one gets a metallic state, while in the case of a large metal–ligand distance, the ground state of the system is nonconducting (Mott–Hubbard insulator).

1.6.4
Indirect Exchange – Double Exchange

In compounds in which magnetic ion occurs in two oxidation states, for example, Fe^{2+} and Fe^{3+} or Mn^{3+} and Mn^{4+}, magnetic coupling may be realized by means of a real electron delocalization to the empty orbital of the neighbor. The hopping of an extra electron of Fe^{2+} or of Mn^{3+} via the O-2p orbital proceeds without the spin-flip of the hopping electron and results in the ferromagnetic coupling of the two centers. This mechanism, called the double exchange, operates in Fe_3O_4, $La_{1-x}Sr_xMnO_3$, or in the Prussian blue, and is associated with increase of conductivity. Such correlation of electric conductivity and ferromagnetism may result in a significant magnetoresistivity.

1.6.5
Indirect Exchange – Antisymmetric Exchange

Energy of the aforementioned exchange interaction does not depend on the direction of spins in the crystal lattice. In the structures where there is no inversion symmetry on the line connecting magnetic ions of spins $\mathbf{S}_1$ and $\mathbf{S}_2$, the spin–orbit interaction in one of them may give rise to the weak anisotropy in the exchange. This contribution is the Dzyaloshinsky–Moriya (DM) interaction equal to

$$\widehat{H}_{\mathrm{DM}} = \mathbf{D}\cdot(\mathbf{S_1} \times \mathbf{S_2}). \tag{1.36}$$

The measure of the DM interaction is the **D** vector, perpendicular to the plane determined by M1, M2, and ligand centers, and proportional to λ, the spin–orbit coupling constant. This interaction tends to align $\mathbf{S}_1$ and $\mathbf{S}_2$ perpendicularly against **D** and against each other and a small canting of magnetic moments may appear. It gives rise to the weak net moment in an antiferromagnet, like in hematite α-Fe_2O_3 or in iron borate $FeBO_3$. Figure 1.5 shows collinear and canted spin arrangements. In general, the DM interaction favors a noncollinear ordering of spins. It influences properties of multiferroics and low-dimensional elements for spintronics.

1.6.6
Itinerant Exchange – RKKY Interaction

Another type of indirect exchange is active in metals, where conduction electrons may mediate the interaction between localized magnetic moments of metal ions (Ruderman, Kittel, Kasuya, and Yosida interaction). This type of coupling applies mainly to lanthanides, in which the 4f shells are localized close to the nucleus. The 4f moments polarize spins of the 5d/6s itinerant electrons and this polarization is transferred to the moment of the adjacent metal ion. The RKKY mechanism depends on a density of states of conduction electrons and works on a long range. The coupling is oscillatory and falls off as r^{-3}

$$J_{\mathrm{RKKY}} \propto \frac{\cos(2k_{\mathrm{F}}r)}{r^3}, \tag{1.37}$$

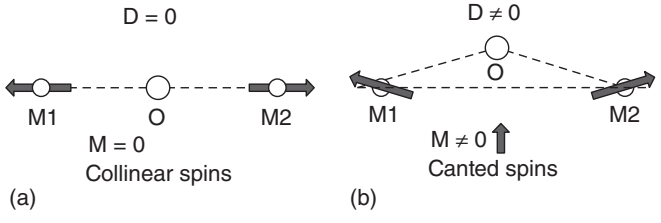

Figure 1.5 (a) Collinear antiferromagnet in case of symmetric exchange; (b) canted moments with weak net magnetization in case of Dzyaloshinsky–Moriya antisymmetric exchange.

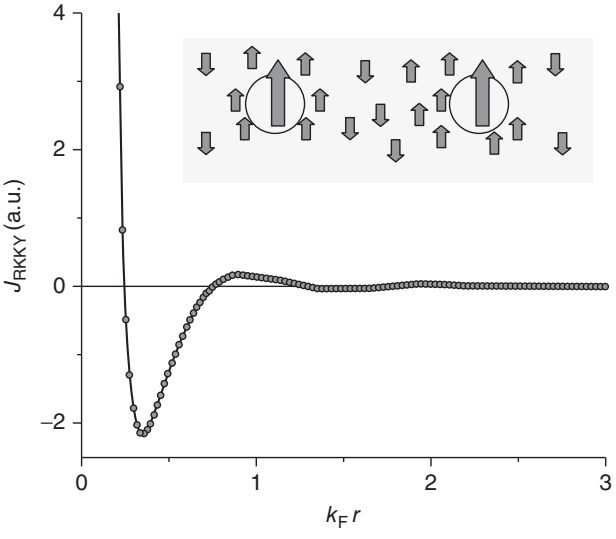

Figure 1.6 RKKY coupling of localized moments mediated by the conduction electrons. The interaction shows an oscillatory behavior.

where k_F is the Fermi wave vector (see Figure 1.6). Depending on the distance between the localized moments of magnetic ions, it may be ferromagnetic or antiferromagnetic. RKKY interaction evokes the long-range magnetic order with the variety of magnetic structures (ferromagnetic and antiferromagnetic, spiral, and helical arrangements). Oscillatory exchange appears also between ferromagnetic layers separated with the nonmagnetic one.

1.6.7
Magnetism of Itinerant Electrons

In the RKKY magnetic interaction, conduction electrons mediate the coupling between the localized moments of the metal ions. Generally, in metals, magnetic moments may come solely from itinerant electrons. Electrons are fermions and occupy all states with wave vector $\mathbf{k}$ within the Fermi sphere $|k| \leq |k_F|$, while the energy of the highest occupied level at $T = 0$ is Fermi energy:

$$E_F = \frac{\hbar^2 k_F^2}{2m_e}. \tag{1.38}$$

The density of states $g(E)$ depends on electron energy as $E^{1/2}$. Due to the Pauli exclusion principle, each state can be occupied with two electrons of opposite spin direction. As shown in Figure 1.7a, in the applied magnetic field, the energy of one sub-band decreases, while it increases for the other. Only electrons from the Fermi level will respond, as only these are able to change spin orientation. Thus, the number of spin-up electrons ($n_\uparrow$) will differ from that of spin-down electrons

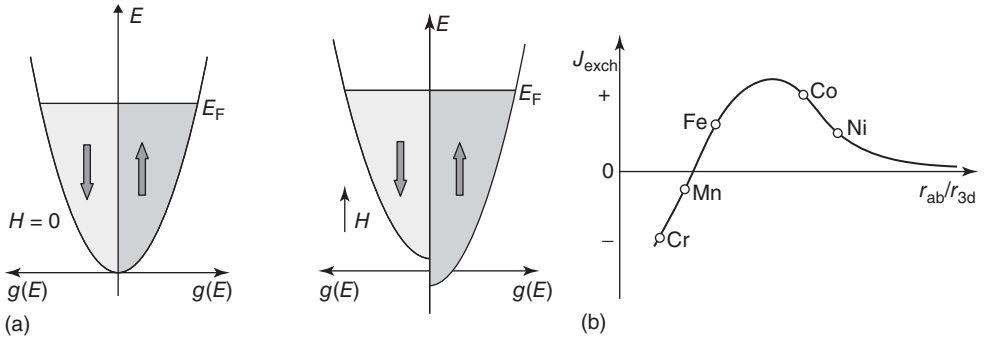

Figure 1.7 (a) Density of states $g(E)$ for itinerant electrons: at $H \neq 0$, the spin sub-bands split, giving rise to Pauli paramagnetism. (b) Relationship between the exchange constant and ratio of the r_{ab} interatomic distance to the radius of the 3d shell. (The Bethe–Slater curve, after [5]).

$(n_\downarrow)$, resulting in a net magnetization

$$M = \mu_B(n_\uparrow - n_\downarrow) = g(E_F)\mu_B^2 B \tag{1.39}$$

and paramagnetic susceptibility, termed as Pauli paramagnetism

$$\chi_{\text{Pauli}} = \mu_0 g(E_F)\mu_B^2 = \frac{3n\mu_0\mu_B^2}{2E_F}, \tag{1.40}$$

where n is the number of electrons per unit volume. Since E_F is about 1 eV ($\sim 10^4$ K), Pauli susceptibility is small and temperature-independent.

As remarked by Landau, besides the Pauli paramagnetism, there is a diamagnetic term due to orbital contribution to the susceptibility. This is, however, weaker than χ_{Pauli}.

The model of a free-electron gas used above is not accurate enough, as it does not account for any interaction between the conduction electrons. However, in transition metals, there is the exchange of the d-band electrons, which is the source of magnetization. Under certain condition, the splitting of the spin-up and spin-down sub-bands can occur spontaneously leading to the ferromagnetism. The condition, known as the Stoner criterion, reads

$$Ug(E_F) \geq 1, \tag{1.41}$$

where U is the Coulomb energy of interaction of the two sub-bands. Among the 3d elements, only iron, cobalt, and nickel fulfill the Stoner criterion and are ferromagnetic. It is mainly due to the large $g(E_F)$ density of states at the Fermi level. On the contrary, as it follows from the Bethe–Slater curve (see Figure 1.7b), ferromagnetism is related to the large ratio of the interatomic distance r_{ab} to the radius r_{3d} of the 3d electron shell. The fingerprint of the band ferromagnetism is a non-integral value of magnetic moment at saturation, $2.22\mu_B$ for Fe, $1.76\mu_B$ for Co and $0.61\mu_B$ for Ni and high Curie temperatures (1043, 1388, and 627 K, respectively). The 4f ferromagnet – Gd, has $T_C = 293.4$ K. Palladium, for which $Ug(E_F)$ is slightly less than 1, exhibits only the enhanced Pauli susceptibility.

1.7
Collective Magnetic State

A sufficiently strong interaction between magnetic moments sets off the spontaneous order of moments below a critical temperature $T_c > 0$. Different types of ordering are met: ferromagnets, antiferromagnets, ferrimagnets, metamagnets, spin glasses, and so on. The study published by Hurd [6] included also magnetic behavior of amorphous systems and superparamagnets. Furthermore, one should also mention systems with reduced dimensions, where shape anisotropy has an essential influence on spin ordering and collective behavior. Magnetic moments in magnets behave in a collective way and the order parameter decreases from the maximum value at $T = 0$ down to zero at $T = T_c$. Exchange interaction, which aligns the spins, is isotropic and does not decide on the orientation of magnetization in the crystal. It is the magnetocrystalline anisotropy, caused by the spin–orbit interaction, which determines an orientation of moments relative to the crystallographic directions. Main types of arrangements of magnetic moments in a bulk magnet are shown in Figure 1.8.

1.7.1
Models of Interaction and Dimension of the Lattice

Bulk magnetic systems are usually described with the Heisenberg model, which assumes magnetic interactions between the nearest neighbors to be entirely isotropic. The Hamiltonian of the magnetic interaction in this case takes the form

$$\hat{H} = -2J_{ex} \sum_{i \neq j} (S_i^x S_j^x + S_i^y S_j^y + S_i^z S_j^z) \tag{1.42}$$

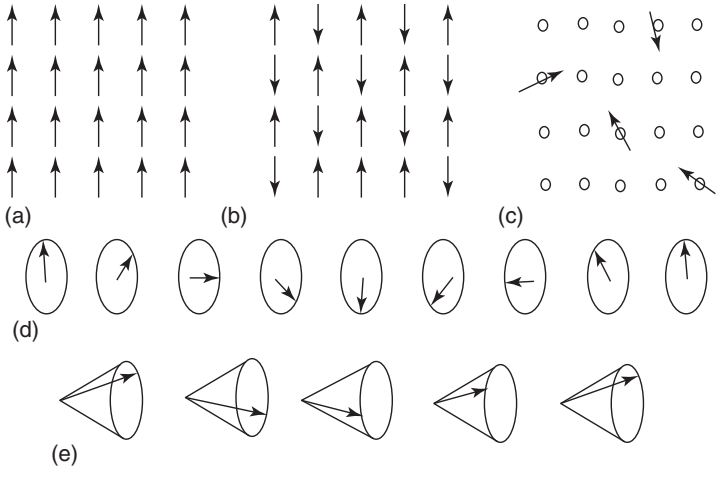

Figure 1.8 Arrangements of magnetic moments in (a) ferromagnet, (b) antiferromagnet, (c) spin glass, (d) helical structure, and (e) spiral structure.

Table 1.2 Occurrence (+) or absence (–) of the long-range order at $T \neq 0$ for dimensions of the lattice and order parameter; ⊗ – Berezinsky–Kosterlitz–Thouless transition.

Model	Dimension of the crystal lattice, d		
	$d = 1$	$d = 2$	$d = 3$
Ising $D = 1$	–	+	+
XY $D = 2$	–	⊗	+
Heisenberg $D = 3$	–	–	+

Source: After [7].

and spins are treated as three-dimensional vectors. Since, generally, the number D of nonzero spin components may differ from three, the following models concern three types of coupling:

a) $D = 3$, Heisenberg model, $\mathbf{S} = [S^x, S^y, S^z]$
b) $D = 2$, XY model, $\mathbf{S} = [S^x, S^y]$
c) $D = 1$, Ising model, $\mathbf{S} = [S^z]$.

A measure of the degree of magnetic ordering below the critical point is the order parameter. A good order parameter is the spontaneous magnetization; in the Ising model, it is a scalar value. The aforementioned spins may reside on the networks of different lattice dimension: $d = 1, 2, 3$. On the basis of the theoretical analysis, it has been found that for the three-dimensional lattice ($d = 3$), the long-range magnetic order at $T \neq 0$ may arise regardless of the dimension D of the order parameter. Magnetic order is periodic, commensurate, or incommensurate to the crystal lattice. In the two-dimensional system ($d = 2$, layer), the long-range order is possible only for the Ising model, while for the XY case, transition to the vortex state is possible (Berezinsky–Kosterlitz–Thouless transition). In the one-dimensional network ($d = 1$, chain), the long-range order beyond $T = 0$ is not possible at all. Table 1.2 provides the summary of these conclusions.

1.7.2 Ferromagnets

The most prominent and important magnetic solids from the application point of view are ferromagnets (e.g., Fe, Co, Ni, Gd, MnSb, EuO, $SmCo_5$, and $Nd_2Fe_{14}B$), the "strongly magnetic" materials, with spontaneous magnetization due to the parallel alignment of spins (Figure 1.8a). Ferromagnetic samples consist of domains in which magnetization reaches its saturation. Orientation of domains and their shapes are governed by the dipolar forces trying to reduce the magnetostatic energy. Orientation of magnetization in the domain depends on the magnetocrystalline anisotropy.

A phenomenological model of ferromagnets was proposed by Weiss within the *molecular field theory* [1, 3]. Magnetic interactions in the ordered systems are represented as an effective field H_{eff} acting on each local moment, in addition to the

external field H. All magnetic ions face the same H_{eff}, which is proportional to the average magnetization M, $H_{\text{eff}} = \lambda M$, where λ is the molecular field constant. Temperature dependence of the magnetization can be calculated by the simultaneous solution of the two equations:

$$M = N_{\text{A}} g_J \mu_{\text{B}} J B_J(y) \tag{1.43}$$

and

$$y = J g_J \frac{\mu_{\text{B}}(H + \lambda M)}{k_{\text{B}} T}, \tag{1.44}$$

where $B_J(y)$ is the Brillouin function defined in Eq. (1.32) and J, g_J, and μ_{B} are the same as defined in Section 1.1. In zero external field, the nonzero magnetization can be obtained below the critical temperature (Curie temperature):

$$T_{\text{C}} = \frac{g_J \mu_{\text{B}} (J+1) \lambda M_{\text{s}}}{3 k_{\text{B}}}. \tag{1.45}$$

The relevant temperature dependence of M/M_{s} at $H = 0$ for different values of total angular momentum J is shown in Figure 1.9. At $T > T_{\text{C}}$, the system is in the paramagnetic state. When the external field is nonzero, magnetization around and above T_{C} grows, while the phase transition disappears. In the limit $H \to 0$ and small value of y argument, the following approximation is valid

$$\frac{M}{M_{\text{s}}} \approx \frac{g_J \mu_{\text{B}} (J+1)}{3 k_{\text{B}}} \left(\frac{H + \lambda M}{T} \right) = \frac{T_{\text{C}}}{\lambda M_{\text{s}}} \left(\frac{H + \lambda M}{T} \right), \tag{1.46}$$

from which an expression for a paramagnetic susceptibility is obtained:

$$\chi = \lim_{H \to 0} \frac{M}{H} = \frac{T_{\text{C}}}{\lambda T \left(1 - \frac{T_{\text{C}}}{T} \right)} = \frac{\frac{T_{\text{C}}}{\lambda}}{T - T_{\text{C}}} = \frac{C}{T - T_{\text{C}}}, \tag{1.47}$$

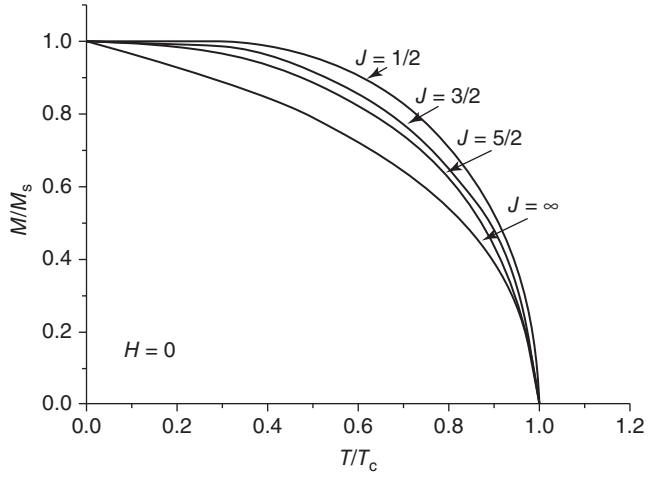

Figure 1.9 Temperature dependence of the relative magnetization M/M_{s} for different values of total angular momentum J. (After [3].)

which is known as the Curie–Weiss law. In general, instead of T_C, a symbol θ is used for the Weiss temperature, which, depending on dimensionality of the lattice and anisotropy, may differ from T_C.

On the basis of the experimentally determined T_C, the molecular field can be estimated. Taking T_C of iron ($\sim 10^3$ K) and $J = 1/2$, one gets $H_{eff} = \lambda M_s \approx 1500$ T, which is an extremely high value. In order to relate it to the exchange integral, we assume that the exchange interaction is active only between the z nearest neighbors and is represented with the integral J_{ex}. From the equation

$$H_{eff} = \frac{2}{g_J \mu_B} z J_{ex} S \tag{1.48}$$

and $M_s = N_A g_J \mu_B J$, we obtain

$$\lambda = \frac{2 z J_{ex}}{N_A g_J^2 \mu_B^2}. \tag{1.49}$$

Thus, in view of Eq. (1.45), T_C is a linear function of the exchange interaction.

A distinctive feature of a large number of ferromagnets is the irreversible (with respect to an imposed magnetic field) process of magnetization and a hysteresis loop (see Figure 1.14a in Section 1.8) [8]. Applying external field H to the unmagnetized material evokes first domain walls motion, while in stronger field, a rotation of magnetization toward the field direction occurs up to saturation at $H = H_s$, when $M(H_s) = M_s$. When H is reduced to zero, magnetization does not vanish, $M(H = 0) = M_R$ (M_R – remanent magnetization), while only at the field H_c (H_c – coercive field) oriented in opposite direction, M disappears. When the applied field is parallel to the so-called *easy axis*, magnetization of saturation is achieved at the smallest H_s. The main term of the anisotropy energy is

$$E_{an} = K_u \sin^2 \varphi, \tag{1.50}$$

where φ is the angle between $\mathbf{M}$ and the easy axis and K_u is the uniaxial anisotropy constant, which depends on the symmetry of the crystal and temperature. The domain walls in strongly anisotropic magnet are narrow, while those in weakly anisotropic magnet are broad. This difference is reflected in the shape of the $M(H)$ curve and the value of H_c, which is proportional to K_u.

1.7.3 Antiferromagnets

In antiferromagnets (e.g., α-Fe_2O_3, Cr_2O_3, CoO, MnO, and $LaFeO_3$), the interaction between magnetic moments is negative and their alignment is antiparallel (Figure 1.8b). Magnetic lattice is divided into two (or more) sublattices in such a way that their net magnetization is zero, that is, $\mathbf{M}_1 = -\mathbf{M}_2$. Molecular field on the sublattices is $H_1 = -|\lambda| M_2$ and $H_2 = -|\lambda| M_1$, with the negative molecular field constant, $\lambda < 0$. Magnetization on each sublattice is given by the same expression as that of a ferromagnet (Eq. 1.45), with $|\lambda|$ instead of λ. The M_1 and M_2 follow the same temperature dependence, and going toward higher temperatures

the long-range magnetic order disappears at the Néel temperature, T_N, which is expressed as

$$T_N = \frac{g_J \mu_B (J+1)|\lambda| M_s}{3k_B}. \tag{1.51}$$

Furthermore, expression for magnetic susceptibility in the molecular field approach is similar to that of a ferromagnet (Eq. 1.46) with the difference that $-T_C$ is replaced by $+T_N$. The Curie–Weiss formula for the susceptibility in the paramagnetic state is common for ferromagnets and antiferromagnets, which is expressed as

$$\chi = \frac{C}{T-\theta}, \tag{1.52}$$

where $\theta > 0$ for ferromagnets and $\theta < 0$ for antiferromagnets.

Figure 1.10 presents the Curie–Weiss law in three forms, i.e. the temperature dependence of χ, χ^{-1} and χ_T, where the last function in the high temperature range (T–θ) is proportional to the square of the effective magnetic moment (see Eq. (1.18)).

Equation (1.52) should be completed with the diamagnetic contribution, especially important for organometallic substances, and with the temperature-independent paramagnetic (TIP) term, allowing for excited states of the system (van Vleck paramagnetism) and/or contribution from free electrons (Pauli paramagnetism). All of these are small and nearly independent on temperature, one uses therefore the modified Curie–Weiss law:

$$\chi = \frac{C}{T-\theta} + \chi_0. \tag{1.53}$$

Magnetic susceptibility of antiferromagnets depends on the direction of the applied field. Field H perpendicular to the sublattice magnetization invokes rotation of M_1 and M_2 against the molecular field and the susceptibility $\chi_\perp$ does not

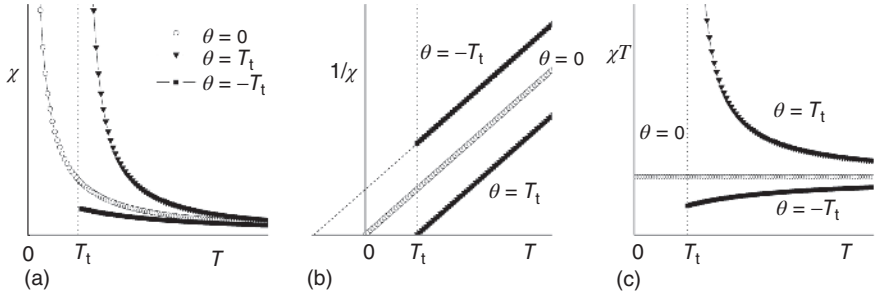

Figure 1.10 Three forms of the Curie–Weiss law for paramagnets: (a) magnetic susceptibility χ, (b) reciprocal susceptibility $1/\chi$, (c) χT. Data of noninteracting moments ($\theta = 0$), ferromagnetic (FM, $\theta = T_t > 0$), and antiferromagnetic (AFM, $\theta = -T_t < 0$) interaction are shown. Transition to the long-range order occurs at the temperature T_t, only paramagnetic region is shown.

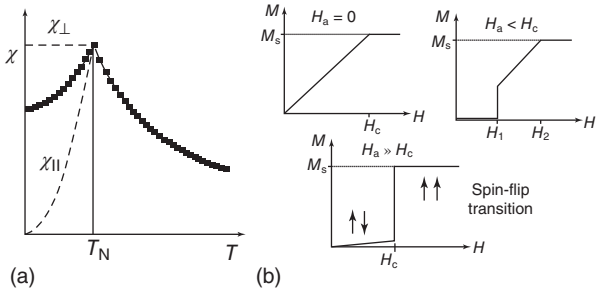

Figure 1.11 (a) Temperature dependence of the magnetic susceptibility for an antiferromagnet (see text). (b) Different types of magnetization curves for an antiferromagnet; H_a is an anisotropy field, H_c is a critical field to reach saturation.

depend on temperature ($\chi_\perp(T) = \chi_\perp(T_N)$). On the contrary, susceptibility in parallel field, $\chi_{||}$, at $T = 0$ is zero and increases with temperature to reach $\chi_\perp$. As shown in Figure 1.11a, for a polycrystalline material, the average value is obtained:

$$\chi_{poly} = \frac{1}{3}\chi_{||} + \frac{2}{3}\chi_\perp. \tag{1.54}$$

Magnetocrystalline anisotropy of the energy about 10^2 times smaller than the exchange influences also a shape of the magnetization curve of an antiferromagnet. Figure 1.11b shows types of magnetization curves for different values of an anisotropy field. Depending on the anisotropy, magnetization of saturation ($M_s = 2M$) may be reached through: (i) gradual rotation of moments against the negative exchange interaction, (ii) reorientation of the spin axis at H_1 followed by rotation (spin flop), or (iii) an abrupt direct reversal of one sublattice (spin flip). The last case presents the field-induced transition to the ferromagnetic state and concerns the systems called *metamagnets*. Metamagnetism is common in the layered compounds (e.g., $FeCl_2$ and $CoCl_2$), where antiferromagnetic interaction occurs between the ferromagnetically coupled layers.

It is important to note that antiferromagnetic order may not only be the collinear one; cancellation of a net moment occurs also for spiral and helical structures, as it takes place in rare earth metals [9].

1.7.4
Ferrimagnets

Ferrimagnet is a system of nonequivalent sublattices coupled by the antiferromagnetic interaction. In the sublattices, values of magnetic moments or the number of magnetic ions may differ and thus the substance will have a net magnetization. Similar to ferromagnets, the ferrimagnetic materials show hysteresis and saturation of magnetization. Due to the different molecular field affecting each sublattice, the temperature dependence of particular sublattices may vary and the resultant moment can show a compensation point at $T_{comp} < T_c$. At $T = T_{comp}$, the total magnetization vanishes, yet for $T > T_{comp}$, it appears and then vanishes at

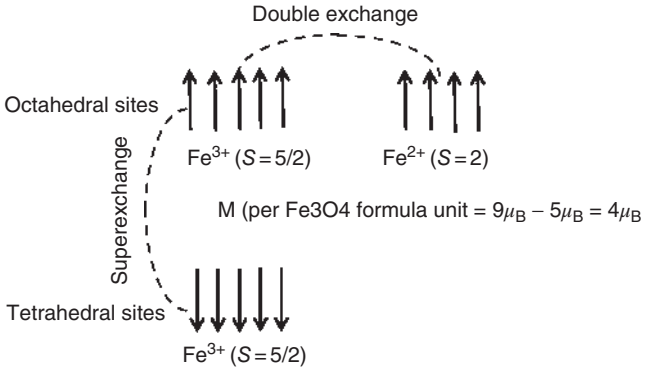

Figure 1.12 Magnetic coupling in ferrimagnetic Fe_3O_4.

$T = T_c$. Susceptibility in the paramagnetic state does not follow the Curie–Weiss law, one can roughly estimate the Weiss temperature θ only from data at $T \gg T_c$.

Ferrimagnetic order appears in a large group of oxides. Ferrites, $MeO{\cdot}Fe_2O_3$ (Me – 3d metal), which are usually insulators, crystallize in the spinel structure. The most famous ferrite is magnetite Fe_3O_4, $T_c = 858$ K, the first-known magnetic material. The Fe^{3+} ions ($S = 5/2$) occupy equally tetrahedral and octahedral lattice sites, while the Fe^{2+} ions ($S = 2$) occupy solely the octahedral sites. The double exchange aligns Fe^{2+} and Fe^{3+} moments in parallel, but the superexchange through the oxygen ligand couples the octahedral and tetrahedral sublattices antiferromagnetically. As shown in Figure 1.12, the net moment comes only from Fe^{2+}. Spinel ferrites show low dependence of magnetization on crystallographic directions, and have low coercive fields.

In ferrimagnets of the garnet cubic structure, $R_3Fe_5O_{12}$ (R is yttrium or rare earth element) or in hexagonal $BaFe_{12}O_{19}$, valence of the iron is Fe^{3+}; however, the number of moments in the tetrahedral sites differs from that in the octahedral sites.

1.7.5
Spin Glasses

In contrast to long-range ordered magnets, spin glasses are the systems in which interactions between the moments of nearest neighbors, both positive and negative, are random. The feature of a spin glass (SG) is disorder and competition of interactions (frustration). Due to frustration, spins have no preferential orientation and the system, as a whole, is not able to simultaneously minimize its energy in the whole volume. Geometric frustration in a triangular or Kagomé lattice with antiferromagnetic interactions leads up to spin fluctuation (spin liquid) and is insufficient for the formation of a spin glass. In turn, a random frustration, connected with a disorder in the occupancy of sites or bonds, leads to the spin glass magnetic collective state below the characteristic freezing temperature, T_f.

First-spin glasses were diluted alloys of a magnetic metal in a nonmagnetic matrix, for example, Cu*Mn* or Au*Fe*. Concentration of a magnetic component is here too low for long-range interactions, but short-range interactions through the conduction electrons are possible. In nonconducting compounds, the spin glass phase appears when positions in a crystal lattice are occupied at random by magnetic and nonmagnetic ions, and ferromagnetic and antiferromagnetic couplings are equivalent, like in $(Eu_{0.80}Sr_{0.20})S$ and $Rb_2Cu_{1-x}Co_xF_4$.

Experimental evidence of the spin glass phase is as follows [10]:

- "Cusp"-shaped anomaly in the differential (AC – *alternating current*) magnetic susceptibility at the freezing temperature T_f; in the limit of the frequency of the AC field $f \to 0$ and $T_f \to T_g$, where T_g is the *glass transition temperature.*
- The "S" shape of the hysteresis loop of magnetization and a small remanence, which decreases with time.
- Dependence of magnetization on the measurement scenario ("history" of the sample): difference in M_{ZFC} (zero-field cooling) and M_{FC} (field cooling) magnetization branches in such a way that (i) the FC branch is reversible and $M_{FC}(T < T_f) = M_{FC}(T = 0)$ and (ii) M_{ZFC} is irreversible and relaxes up to M_{FC}.

Due to the competition of magnetic interactions, dynamics of magnetization in spin glasses is complex. An important feature is a wide distribution of relaxation times and a dramatic increase of the average relaxation time upon cooling. It was found that the temperature T_f of the "cusp" anomaly observed in the AC susceptibility measurements depends on the frequency f of the alternating field and increases with f according to the Vogel–Fulcher formula:

$$f = f_0 \exp\left(-\frac{E_a}{T_f - T_0}\right), \tag{1.55}$$

where $f_0 \approx 10^{13}$ s, E_a is the activation energy, and T_0 describes the interaction between the spin clusters formed during the cooperative SG transition.

The mean field model of the spin glass formulated by Sherrington and Kirkpatrick [11] concerns an infinite Ising spin system. In this approach, distribution of exchange interactions is given by J_0 – the average exchange integral and ΔJ – the exchange deviation. As shown in Figure 1.13a, dependent on the $J_0/\Delta J$ ratio, three possible transitions on the temperature decrease are expected:

i. paramagnet → spin glass (P → SG)
ii. paramagnet → ferromagnet (P → FM)
iii. the twofold transition: paramagnet → ferromagnet → spin glass (*reentrant spin glass* – RSG)

The analysis of the SG phase diagram in the applied magnetic field has shown that the temperature of the paramagnet → spin glass transition decreases with the field increase according to $T_f(H = 0) - T_f(H \neq 0) \approx H^{2/3}$. This is the so-called de Almeida–Thoules irreversibility line. In general, two irreversibility lines are possible: the one for freezing transverse spin components (Gabay–Toulouse line) and the other for freezing the longitudinal spin components of the field dependence given above (see Figure 1.13b).

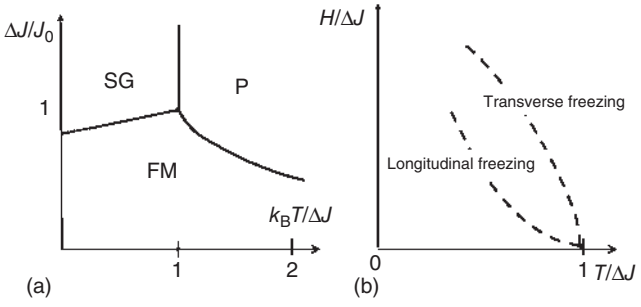

Figure 1.13 (a) Schematic Sherrington–Kirkpatrick phase diagram; (b) $H-T$ mean field phase diagram for spin glass showing the freezing lines of longitudinal and transverse spin components (for details, see text).

1.7.6
Superparamagnets

Superparamagnetic properties arise when the size of the magnetic particles is reduced down to the critical value $d_s \approx 2J_{ex}{}^{1/2}/M_s$ ($d_s \approx 1-100$ nm) when division into domains would not lower the energy. Thus, the particle is the single-domain and has an enormous magnetic moment of $\geq 10^3 \mu_B$. There is no hysteresis when the system gets magnetized and the $M(H)$ curves measured at different temperatures as the function of H/T are the same. Magnetic susceptibility at high temperatures follows the Curie law, like in paramagnets but on the temperature decrease it stops and at the so-called blocking temperature, T_B, falls down to zero. Such behavior is due to the strong increase in the response time of the sample to the magnetic field change.

Let us analyze the temperature dependence of the relaxation time for the single-domain particle. Due to the magnetocrystalline anisotropy or shape anisotropy, only up and down orientations of magnetization are possible. The energy barrier ΔE for the orientation change is a product of the anisotropy constant K and particle volume V. Relaxation of magnetization is exponential ($M(t) = M(0)\exp\left(\frac{t}{\tau}\right)$) and is thermally activated, therefore magnetization changes at high temperatures are quicker but slow down on cooling. The relaxation time is given by

$$\tau = \tau_0 \exp\left(\frac{\Delta E}{k_B T}\right) = \tau_0 \exp\left(\frac{KV}{k_B T}\right), \tag{1.56}$$

where $\tau_0 \sim 10^{-9}$ s. The value of τ depends not only on temperature, but also on the volume and anisotropy of the particles. For example, the relaxation time of the cobalt particle of diameter 6 nm at room temperature is $< 10^{-1}$ s, while in case of 12-nm diameter it is about 1 year. Experimental methods used to investigate magnetic relaxation (magnetometry, Mössbauer, neutron scattering, muon spin rotation, etc.) operate in different time windows. If one assumes $\tau = 100$ s as an upper limit of the experimental observation time, then the exponent in Eq. (1.56) is $KV/k_B T = 25$, while the temperature for which the relaxation time

of the given particle would exceed 100 s, will be called the blocking temperature $T_B = KV/25k_B$. At $T < T_B$, magnetic moments of the particles are in the blocked state and magnetization is irreversible (hysteresis loop). At $T > T_B$, the particles are in the superparamagnetic state, magnetization is reversible, and there is no hysteresis loop. Detailed analysis of the relaxation for an exact system of particles is a complex task. Different mechanisms of relaxation have to be allowed and the distribution of particle size, as well as a possible interparticle coupling should be taken into account.

1.8 Applications and Research

Magnetic materials are used in numerous and miscellaneous applications. The benchmark for using a given material is the shape of the hysteresis loop measured at room temperature. Materials with highest ordering temperatures are of the main interest. Figure 1.14a shows schematically the $M(H)$ dependence for a ferromagnet (or ferrimagnet), where M_s is the magnetization of saturation, M_R is the remanence, and coercivity H_c is the reverse field needed to bring down magnetization to zero. The M_s is an intrinsic feature that reveals the spontaneous magnetization, which exists within a domain of a ferromagnet. The M_R and H_c are the extrinsic properties, which depend on the microstructure of the sample, size of grains, defects, thermal history, and field-sweeping rate. The area under the full hysteresis loop is a measure of the energy needed to reverse the magnetization. Dependent on the shape of the loop, two main categories of magnetic materials are defined: soft magnets (easy to magnetize and demagnetize, small energy dissipated) and hard magnets (large energy dissipated). Soft magnetic materials have small magnetocrystalline anisotropy and small coercivity field ($H_c < 125$ Oe) and

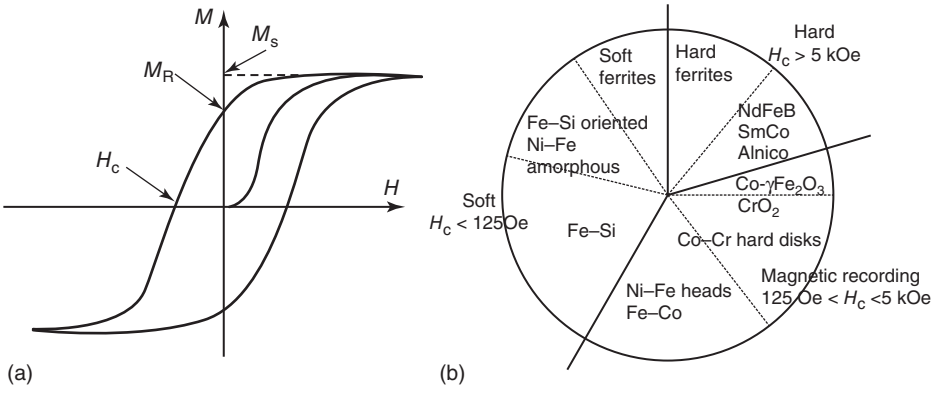

Figure 1.14 (a) Schematic shape of a hysteresis loop: M_s – magnetization of saturation, M_R – remanence, and H_c – coercivity; (b) approximate market share of the main types of applied magnetic materials. (After [3].)

are used in transformer cores, motors, and generators. A standard soft magnet is the nickel–iron alloy called permalloy with $H_c \approx 10^{-2}$ Oe.

Hard magnets, referred as permanent magnets, have large coercive field $H_c > 5$ kOe due to large anisotropy and domain wall pinning. Due to large remanence, they generate magnetic field and are used in motors, generators, loudspeakers, actuators, and holding devices. The important materials here are ferrites, for example, $Ba_2Fe_{12}O_{19}$, or rare earth compounds, such as Sm–Co alloys or $Nd_2Fe_{14}B$ with H_c of about 12 kOe. Materials with an intermediate coercive field, $125\,\text{Oe} < H_c < 5$ kOe, are used for magnetic recording. Fine particles of Fe or Co-doped γ-Fe_2O_3 are used for flexible recording media, while thin films of Fe–Ni or Fe–Co alloys are applied in write/read heads. An approximate market share of main types of applied magnets is shown in Figure 1.14b.

In order to achieve the best performance materials, investigation of the effect of microstructure, grain boundaries, texture, and other factors of magnetization reversal processes are performed. It appears that mixed multiphase and/or nanostructured magnets may offer new, promising properties. Research on "stronger, lighter, and more energy-efficient" magnetic materials has been reviewed [12].

It is known that ferromagnetic materials may show a considerable change of various physical properties upon an applied magnetic field. There are magnets showing magnetoelastic, magnetocaloric, magneto-optic, magnetoelectric, and magnetotransport effects, which may be used as sensors. Of special importance is a phenomenon of a giant magnetoresistance (GMR) appearing in magnetic/nonmagnetic multilayers coupled by the RKKY interaction. They are used in hard disk drives and random-access memory cells, which have significantly increased the density of information stored. GMR is explained in terms of two components (with spin-up and spin-down) of electric current. It assumes different mobilities, mean free paths, and hence different resistances of the components, which decrease the resistivity of the field-aligned multilayers.

Magnetic nanoscale materials also show other interesting effects in addition to the GMR. When at least one of the dimensions is diminished down to nanometers (1–100 nm), that is, a characteristic magnetic or electrical length scale, changes in anisotropy, remanence, Curie point, conductivity, and other properties occur. Investigation of nanostructured magnets is a very active area of research. Stacks of thin films are the base of modern magnetic sensors and memory elements; systems with two nanoscale dimensions are nanowires or nanorods, which may be used in electronics, magnetic recording, or biomedicine; if all three dimensions are confined down to nanometers, one deals with superparamagnetic nanoparticles (see above), widely applied as magnetic recording media and in medicine for diagnostics and targeted therapy. Related to the nanoscale magnetism is magnetism of the molecule-based materials, an important and promising interdisciplinary area of research [13].

Discovery of GMR entered a new, interdisciplinary field of research – spintronics. Spintronics joins magnetism with electronics, in contrast to conventional electronics, dealing solely with the electron charge. It is believed that manipulating spin polarization of mobile electrons by means of magnetic field will

offer an enhanced functionality, higher speed, and reduced power consumption of the devices [14]. Materials used in spintronics are films of conventional 3d metals and alloys, half-metals with electrons of only one spin polarization at the Fermi level such as CrO_2 or $La_{1-x}Sr_xMnO_3$ (LSMO). It was found that spin lifetimes and diffusion lengths are much longer in semiconductors than they are in metals [3]. Another interesting and successful approach is using organic [15, 16] and molecular [17] components into spintronic systems. The important features of the spin transport in organic and molecular materials are convenient values of the spin diffusion length and the spin relaxation time due to the very small spin orbital coupling in carbon-based compounds.

References

1. Blundell, S. (2001) *Magnetism in Condensed Matter*, Oxford University Press, New York.
2. Getzlaff, M. (2008) *Fundamentals of Magnetism*, Springer-Verlag, Berlin, Heidelberg.
3. Coey, J.M.D. (2009) *Magnetism and Magnetic Materials*, Cambridge University Press, Cambridge.
4. Bloch, D. (1963) *J. Phys. Chem. Solids*, **27**, 881–885.
5. Goodenough, J.B. (1963) *Magnetism and the Chemical Bond*, Wiley-Interscience, New York.
6. Hurd, C.M. (1982) *Contemp. Phys.*, **23**, 469–493.
7. (a) De Jongh, L.J. and Miedma, A.R. (1974) *Adv. Phys.*, **23**, 1–260; (b) De Jongh, L.J. and Miedma, A.R. (2001) *Adv. Phys.*, **50**, 947–1170.
8. Chikazumi, S. (1997) *Physics of Ferromagnetism*, Oxford University Press, New York.
9. Koehler, W.C. (1965) *J. Appl. Phys.*, **36**, 1078–1087.
10. Mydosh, J.A. (1993) *Spin Glasses: An Experimental Introduction*, Taylor & Francis, London.
11. Sherrington, D. and Kirkpatrick, S. (1975) *Phys. Rev. Lett.*, **35**, 1792–1796.
12. Gutfleisch, O., Willard, M.A., Brück, E., Chen, C.H., Sankar, S.G., and Liu, J.P. (2011) *Adv. Mater.*, **23**, 821–842.
13. Benelli, C. and Gatteschi, D. (2015) *Introduction to Molecular Magnetism: From Transition Metals to Lanthanides*, Wiley-VCH Verlag GmbH, Weinheim.
14. Hirohata, A. and Takanashi, K. (2014) *J. Phys. D: Appl. Phys.*, **47**, 193001.
15. Sugawara, T. and Matsushita, M.M. (2009) *J. Mater. Chem.*, **19**, 1738–1753.
16. Szulczewski, G., Sanvito, S., and Coey, M. (2009) *Nat. Mater.*, **8**, 693–695.
17. Camarero, J. and Coronado, E. (2009) *J. Mater. Chem.*, **19**, 1678–1684.
18. Drillon, M., Panissod, P., Rabu, P., Souletie, J., Ksenofontov, V., and Gütlich, P. (2002) *Phys. Rev. B*, **65**, 104404.